Introducing a high throughput nanocatalytic method toward the synthesis of some pyrazolo phthalazine derivatives under green conditions utilizing imidazoliume based ionic liquid supported on the silica-coated nanosized perlite as a novel, reusable and eco-friendly nanocatalyst

Leila Moradi[1] · Hamideh Rouhi Sasi[1] · Abdulhamid Dehghani[1]

Abstract

A high throughput ionic liquid-based catalytic system as a new efficient and reusable heterogeneous nanocatalyst was developed for the one-pot synthesis of some 1H-pyrazolo [1,2-b] phthalazine-5,10-diones in ethanol at 78 °C. The designed nanocatalyst was synthesized and then characterized for their functionality, composition, size, morphology, surface properties, and crystalline size by Fourier-transform infrared spectroscopy (FTIR), Energy dispersive X-ray, Transmission electron microscopes, Field emission scanning electron microscopy, Brunauer–Emmett–Teller, and X-Ray diffraction techniques. The target products were obtained in high to excellent yields (80–96%) in this protocol. The structure of all synthesized products was determined via hydrogen nuclear magnetic resonance (^{1}H NMR) and FT-IR spectra. This eco-friendly method has advantages such as a clean reaction profile, low amount of the catalyst, mild reaction conditions, environmentally benign solvent, short reaction times and high to excellent yield of products. Moreover, there is no remarkable loss in the catalytic activity of perlite NPs/SiO$_2$/IL after six cycles of reuse. Also, the results of hot filtration studies show that leaching is not occur in catalyst surfaces and prove the complete heterogeneous behavior of perlite NPs/SiO$_2$/IL under optimized reaction conditions.

✉ Leila Moradi
l_moradi@kashanu.ac.ir

1   Department of Organic Chemistry, Faculty of Chemistry, University of Kashan, P.O. Box 8731753153, Kashan, Iran

Graphical Abstract
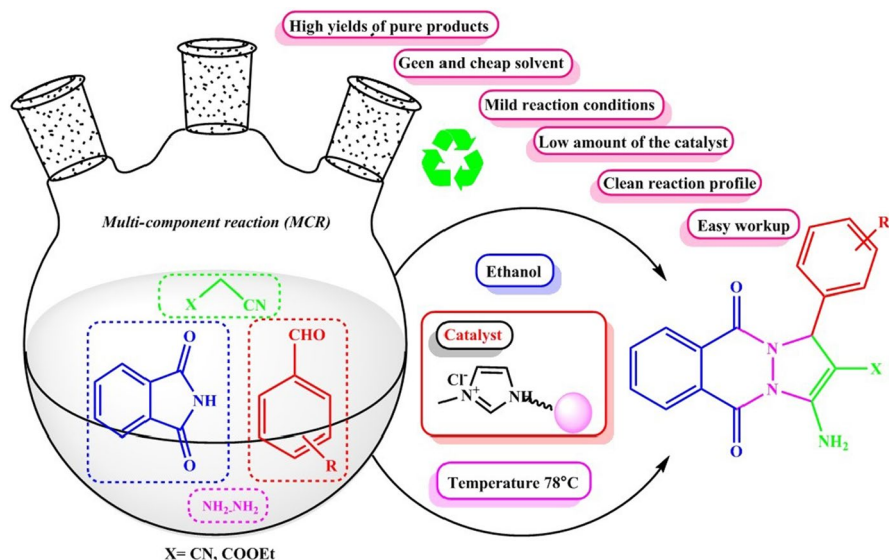
Introduction

The most complex branches of chemistry are usually the chemistry of heterocyclic compounds, which is one of the widespread classical divisions of organic chemistry. Literature review shows that more than 85–95% of new drugs contain heterocyclic compounds [1–3]. In recent decades, N-containing heterocycles have been widely used as novel scaffolds for drug discovery. Therefore, N-heterocycles play an important role in biological and pharmaceutical research. Coenzymes, nucleic acids, vitamins, enzymes, alkaloids and hormones are contained in N-based heterocycles as scaffolds. Metronidazole, chlorpromazine, diazepam, metronidazole, captopril, and azidothymidine are among the most well-known drugs based on nitrogen-containing heterocyclic rings [4–11].

Among biologically important nitrogen-containing heterocyclic compounds, phthalazine cores are of significant importance due to their presence in biologically active compounds and drugs [12–14]. Phthalazines, also called benzo-orthodiazines or benzopyridazines are a variety of bicyclic heterocycles in which the benzene rings are fused to 6-membered heterocycles containing two nitrogens, and finally, it is introduced as an interesting nucleus, which has many medicinal properties and

biological activities. Phthalazines are structural isomers of naphthyridines such as quinazoline and quinoxaline [15–17]. Pyrazolo[1,2-b]phthalazine-diones are an important group of phthalazine compounds, which have some biological activity. These compounds have analgesic, anti-hypoxic, anti-seizure, anti-inflammatory, anti-allergic, and anti-hyperglycemic activities [18–23]. Due to the wide biological applications of phthalazine derivatives, much interest has been directed towards the development of more efficient protocols for the synthesis of these compounds. A common approach for the synthesis of pyrazolo[1,2-b]phthalazine-diones nucleus generally involves multicomponent reactions of phthalimide, hydrazine hydrate, malononitrile, and various aryl aldehydes in the presence of a catalyst. The importance of multi-component reactions in this synthesis can be mentioned for easy implementation, short response time, high atomic yield, high variety of products, and easy purification. To date, several reports have been published on the one-pot synthesis of Pyrazolo[1,2-b]phthalazine-diones using homogeneous and heterogeneous catalysts. However, some of these reported methods for the synthesis of Pyrazolo[1,2-b]phthalazine-diones have low yields as well as long reaction times and the use of homogeneous acids as catalysts [24–36]. As a result, safer synthetic methods with shorter reaction times and higher efficiency are considered, which can be done by using new and efficient catalysts.

Nowadays, the goal of many chemists is to focus on development of the new efficient, inexpensive, easily separable heterogeneous catalytic systems for the synthesis of heterocyclic and medicinal compounds. Green chemistry is driving the industry to implement innovative purifications involving the use of alternative heterogeneous catalytic processes [37–42].

Perlite or pearl stone is a type of rhyolite or in other words a natural glass with concentric cracks, whose refractive index and specific gravity are similar to obsidian. Perlite is a non-crystalline glass and an organic dust material with a typical composition of 70–75% silicon dioxide, 12–15% aluminum oxide, 3–5% potassium oxide, 3–4% sodium oxide and traces amounts of iron oxide, magnesium oxide and calcium oxide. The porous nature of perlite, as well as its very low density, has led to its use as a good thermal acoustic insulation for cavity walls and a valuable low-density fireproofing additive, and can also be a suitable substitute for sand in light-weight plaster and concrete aggregates. Prior to about 1950, perlite was virtually unknown in the trade. Other uses of perlite include water purification in urban swimming pools, as well as an abrasive agent in polishes, cleaners and soaps [43–45]. In addition, perlite has been found to be an excellent support for the stabilization of biocatalysts [46] In recent years, several reports have been published on the heterogeneous synthesis of pearlite-based catalysts [47–50].

In the last few decades, green chemistry has provided alternative safe routes for synthesis. Among the investigated methods, great attention has been paid to ionic liquids and recently these compounds have attracted increasing attention in the field of green organic synthesis. The high number of articles published in relation to them is proof of this claim, although more than a century has passed since the recognition of ionic liquids [51–54]. In 1818, ethyl ammonium nitrate was reported as the

first ionic liquid by Gabriel and Wiener. Ionic liquids or molten salts are a group of chemical compounds which are prepared by placing organic cations and inorganic anions together. Each cation and anion give special properties to ionic liquids according to their type and size, so by changing the type of cations and anions, their properties can be changed and adjusted, hence, ionic liquids are also called to be designer solvents [55–60]. Ionic liquids are an interesting and valuable family that were initially introduced as alternative green reaction media, but today they play an important role in controlling reactions as solvents or catalysts [61–63]. Ionic liquids are introduced as green and environmentally friendly solvents due to their high thermal and chemical stability, high viscosity, low vapor pressure, and favorable solvent coverage [64, 65]. Many organic reactions such as Diels–Alder and Friedel–Crafts reactions can be performed with the help of ionic liquids. One of the most attractive applications of ionic liquids or molten salt is the synthesis of materials, including nanomaterials. In addition, ionic liquids can catalyze reactions in chemistry. Many organic reactions have been performed in ionic liquids as catalysts with excellent results. Catalytic reactions have been carried out in ionic liquid environments for nearly three decades, and the first report of using ionic liquids as a catalyst can be attributed to the Friedel–Crafts acylation reaction in 1986. Among other features of ionic liquids as a catalyst, we can mention their ability to be recycled and reused in reactions [66–70]. It should be noted that by adjusting the components of ionic liquids, the stability, size and solubility of nanoparticles can be adjusted. In addition, the effect of ionic liquids on catalyst nanoparticles is particularly important, these materials prevent the accumulation of nanoparticles by covering the electrically charged layers on the surface of colloids, and then it causes the stability and stabilization of the system [71–73].

In the present study, the methylimidazole based ionic liquid (IL) supported on the silica-coated perlite nanoparticles (Perlite NPs/SiO$_2$/IL) was prepared. Then, we disclosed a novel methodology for the synthesis of 1H-pyrazolo [1,2-b] phthalazine-5,10-diones by condensation of phthalimide, hydrazine hydrate, various aryl aldehydes and malononitrile in the presence of perlite NPs/SiO$_2$/IL under thermal conditions.

Experimental section

All required chemicals were purchased from basic chemical companies. Products were purified by recrystallization from appropriate solvents and identified by their melting point, ^{1}H NMR, and FT-IR analyzer subsequently. ^{1}H NMR spectra were recorded on a Brucker Avance DPX-400 (^{1}H NMR 400 MHz) spectrometer in pure deuterated dimethylsulfoxide (DMSO-d$_6$). Chemical shifts are given in parts per million (ppm) downfield from tetramethylsilan as an internal reference and coupling constants (*J*-values) are in hertz (Hz). Fourier-transform infrared spectra were obtained as KBr pellets with a Nicolet Magna series FT-IR 550 spectrophotometer for the characterization of the products. X-ray diffraction patterns of catalysts were recorded by the Bruker AXS

D8-advance X-ray diffractometer using CuKα radiation ($\lambda = 1.54178$ Å) with scanning range 2θ from 10° to 80°. The catalysts were characterized by Field Emission Scanning Electron Microscopy (Sigma ZEISS) performed at an accelerating voltage of 15 kV. Transmission electron microscopy (TEM) images were recorded using a Philips EM 208S instrument with an accelerating voltage of 100 kV. The Brunauer- Emmett-Teller (BET) surface area analysis was adopted at 77 K to obtain surface areas with Belsorp mini II apparatus (Microtrac Bel Corp, Japan) after the sample had been degassed in a flow of N_2. To evaluate the thermal decomposition of the individual component and their mixture, Thermogravimetric Analysis (TGA) was performed on a PerkinElmer device manufactured by Thermal Sciences. Melting points were specified on a Scientific Thermo oil heated melting point system (model, 9100 BZ; United Kingdom).

Synthesis of perlite NPs

Perlite NPs were prepared according to the procedure reported in the literature [18]. In brief, 5 g of crystalline form of perlite was calcined at 500 °C for 1 h, followed by adding HCl (150 mL, 2 M). Afterwards, the reaction mixture was stirred magnetically under reflux conditions for about 24 h. After the time, the obtained precipitate was collected and washed with distilled water (3*30 mL). Finally, the product was calcined at 700 °C for 2 h and Perlite NPs was obtained as a white solid powder.

Synthesis of perlite/SiO$_2$

In a typical procedure, the prepared perlite nanoparticles (2.0 g) were dispersed in a mixture of ethanol (80 mL), DI-water (20 mL), and tetraethoxysilane (TEOS) (1 mmol, 0.2 g). Afterwards, 2 mL of NaOH (10 wt %) was added dropwise. After being refluxed for 24 h at ambient temperature, the precipitate was collected and washed with ethanol (2*30 mL) and DI-water (2*30 mL) and dried at 60 °C.

Synthesis of perlite/SiO$_2$ decorated with 3-chlorotrimethoxypropyl silane (Perlite/CPTES)

To a 100 mL round-bottom flask containing 22 mL of tetrahydrofuran, perlite NPs/SiO$_2$ (1.5 g) was added and truly dispersed under ultrasonic irradiation. After that, 3-chloromethoxypropylsilane (20 mmol, 4 g) was added and the resulting mixture was then set to be refluxed with stirring for 16 h at 80 °C. Then, the obtained solid was collected and washed with ethanol (2*20 mL), DI-water (2*20 mL) and dried at 60 °C for 12 h.

Synthesis of perlite/SiO$_2$/IL

Eventually, 1.0 g of Perlite NPs/CPTES was dissolved in toluene (8.0 mL), which was sonicated for 10 min followed by adding 4 mmol (0.3 g) of methylimidazole. The

mixture was refluxed for 24 h at 90 °C. After the completion of the reaction, the precipitate was washed with ethanol (2*10 mL) and dried at 60 °C for 48 h.

General procedure for the preparation of 1H-pyrazolo[1,2-b] phthalazine-5,10-dione derivatives

The 100 mL round bottom flask was charged with phtalimide (**1**, 1 mmol), hydrazinehydrate (**2**, 1 mmol), and the catalyst (0.02 g) in ethanol (2.0 mL). The reaction mixture was stirred under heating conditions at 78 °C and the progress of reaction was monitored by TLC to obtain the phtalhydrazide. Afterwards, aldehyde derivative (**3**, 1 mmol) and ethyl cyanoacetate or malononitrile (**4**, 1 mmol) was added and vigorous stirring continued until the reaction was completed (monitored by TLC). Then, the reaction mixture was immediately poured to the cold methanol (10 mL) and the resulting precipitate was filtered, washed with ethanol and recrystallized from ethanol to afford the pure product (**5d**).

Spectral data

Compound 5a: Yield: 96%, yellow powder; Mp. 274-276 °C (lit. 272-274 °C) [74]; FTIR (ν_{max}, cm^{-1}) 3431–3019 (NH$_2$ stretch), 2196 (CN stretch), 1659 (C=O stretch), 1599–1378(arom. C=C stretch); ^{1}H NMR (400 MHz, DMSO-d_6) δ (ppm) 7.24–7.05 (m, 5H, NH$_2$, aromatic), 7.94 (s, 2H, aromatic), 7.76 (t, 3H, J = 9.0 Hz, aromatic), 6.26 (s, 1H, CH).

Compound 5b: Yield: 95%, yellow powder; Mp. 269-271 °C (lit. 268-270 °C) [75]; FTIR (ν_{max}, cm^{-1}) 3361–3244 (NH$_2$ stretch), 2197 (CN stretch), 1663 (C=O stretch), 1603–1407 (arom. C=C stretch); ^{1}H NMR (400 MHz, DMSO-d_6) δ (ppm) 8.42–8.06 (m, 6H, NH$_2$, aromatic), 8.01–7.69 (m, 2H, aromatic), 7.67 (t, 2H, J = 8.0Hz, aromatic), 6.33 (s, 1H, CH).

Compound 5c: Yield: 83%, yellow powder; Mp. 258-260 °C (lit. 259-261 °C) [76]; FTIR (ν_{max}, cm^{-1}) 3371–3256 (NH$_2$ stretch), 2190(CN stretch), 1657(C=O stretch), 1608–1437 (arom. C=C stretch); ^{1}H NMR (400 MHz, DMSO-d_6) δ (ppm) 8.24–7.94 (m, 6H, NH$_2$, aromatic), 7.37 (d, 2H, J = 8.0 Hz, aromatic), 6.9 (d, 2H, J = 8.0Hz, aromatic), 6.08 (s, 1H, CH), 3.74 (s, 3H, OMe).

Compound 5d: Yield: 88%, yellow powder; Mp. 271-273 °C (lit. 272-274 °C) [77]; FTIR (ν_{max}, cm^{-1}) 3360–3258 (NH$_2$ stretch), 2197 (CN stretch), 1658 (C=O stretch), 1568–1437 (arom. C=C stretch); ^{1}H NMR (400 MHz, DMSO-d_6) δ (ppm) 8.25–7.93 (m, 7H, NH$_2$, aromatic), 7.38–6.89 (m, 4H, aromatic), 6.51 (s, 1H, CH).

Compound 5e: Yield: 83%, yellow powder; Mp. 245-247 °C (lit. 247-249 °C) [44]; FTIR (ν_{max}, cm^{-1}) 3361–3260 (NH$_2$ stretch), 2194(CN stretch), 1658(C=O stretch), 1606–1437(arom. C=C stretch); ^{1}H NMR (400 MHz, DMSO-d_6) δ (ppm) 8.26–7.94 (m, 6H, NH$_2$, aromatic), 7.25–7.11(m, 4H, aromatic), 2.28(s, 3H, Me).

Compound 5f: Yield: 84%, yellow powder; Mp. 251-253 °C (lit. 250-252 °C) [75]; FTIR (ν_{max}, cm^{-1}) 3362–3260(NH$_2$ stretch), 2196(CN stretch), 1657(C=O stretch), 1567–1437(arom. C=C stretch); ^{1}H NMR (400 MHz, DMSO-d_6) δ (ppm) 8.21–7.58 (m, 6H, NH$_2$, aromatic), 7.30 (d, 2H, J = 7.6Hz, aromatic), 7.13 (d, 2H, J = 7.2Hz, aromatic), 6.05 (s, 1H, CH), 1.92 (s, 3H, Me).

Compound 5g: Yield: 85%, yellow powder; Mp. 250-253 °C (lit. 250-252 °C) [78]; FTIR (ν_{max}, cm^{-1}) 3372–3173(NH$_2$ stretch), 2209(CN stretch), 1656(C=O stretch), 1611–1437(arom. C=C stretch); ^{1}H NMR (400 MHz, DMSO-d_6) δ (ppm) 8.13–7.86(m, 8H, NH$_2$, aromatic), 7.59–7.32 (m, 4H, aromatic), 6.45(s, 1H, CH).

Compound 5h: Yield: 84%, yellow powder; Mp. 267-269 °C (lit. 268-270 °C) [78]; FTIR (ν_{max}, cm^{-1}) 3375–3263 (NH$_2$ stretch), 2199(CN stretch), 1660 (C=O stretch), 1563–1439 (arom. C=C stretch); ^{1}H NMR (400 MHz, DMSO-d_6) δ (ppm) 8.25–7.94 (m, 6H, NH$_2$, aromatic), 7.52.7.40 (m, 4H, aromatic), 6.13(S, 1H, CH).

Compound 5i: Yield: 80%, yellow powder; Mp. 256-258 °C (lit. 255-257 °C) [26]; FTIR (ν_{max}, cm^{-1}) 3363–3240(NH$_2$ stretch), 2400(CN stretch), 1659(C=O stretch), 1653–1428(arom. C=C stretch); ^{1}H NMR (400 MHz, DMSO-d_6) δ (ppm) 8.28.7.97 (m, 6H, NH$_2$, aromatic), 7.68–7.40 (m, 3H, aromatic), 6.43(S, 1H).

Compound 5j: Yield: 87%, yellow powder; Mp. 257-259 °C (lit. 259-261 °C) [79]; FTIR (ν_{max}, cm^{-1}) 3382–3253(NH$_2$ stretch), 2199(CN stretch), 1659(C=O stretch), 1564–1424(arom. C=C stretch); ^{1}H NMR (400 MHz, DMSO-d_6) δ (ppm) 8.27–7.97(m, 6H, NH$_2$, aromatic), 7.30–6.88(m, 4H, aromatic), 6.33(s, 1H, CH), 2.49(s, 3H, OCH$_3$).

Compound 5k: Yield: 88%, yellow powder; Mp. 146-148 °C (lit. 152-154 °C) [77]; FTIR (ν_{max}, cm^{-1}) 3372–3294(NH$_2$ stretch), 2185(CN stretch), 1658(C=O stretch), 1602–1438(arom. C=C stretch); ^{1}H NMR (400 MHz, DMSO-d_6) δ (ppm) 8.62–7.92(m, 5H, aromatic), 7.05–6.90(m, 4H, aromatic), 6.06(s, 1H, CH), 3.73(s, 3H, OMe), 3.71(S, 3H, OMe).

Compound 5l: Yield: 88%, yellow powder; Mp. 241-243 °C (lit. 242-244 °C) [80]; FTIR (ν_{max}, cm^{-1}) 3376–3258 (NH$_2$ stretch), 2200 (CN stretch), 1651(C=O stretch), 1566–1440(arom. C=C stretch); ^{1}H NMR (400 MHz, DMSO-d_6) δ (ppm) 8.23–7.95(m, 6H, NH$_2$, aromatic), 7.53–7.01(m, 3H, aromatic), 6.51(s, 1H, CH).

Compound 5m: Yield: 91%, yellow powder; Mp. 239-241 °C (lit. 239-241 °C) [81]; FTIR (ν_{max}, cm^{-1}) 3434–3256(NH$_2$ stretch), 1697(C=O), 1656(C=O stretch), 1437–1608(arom. C=C stretch;^{1}H NMR (400 MHz, DMSO-d_6) δ (ppm) 8.29–7.96(m,6H, NH$_2$, aromatic), 7.90–7.73(m, 4H, aromatic), 6.13(s, 1H, CH), 4.01–3.94(q, 2H, J = 7.2Hz, CH$_2$), 1.03(t, 3H, J = 7.2Hz, Me).

Compound 5n: Yield: 89%, yellow powder; Mp. 235-237 °C (lit. 236-238 °C) [82]; FTIR (ν_{max}, cm^{-1}) 3425–3382(NH$_2$ stretch), 1694(C=O stretch), 1652(C=O stretch), 1610–1434(arom. C=C stretch); ^{1}H NMR (400 MHz, DMSO-d_6) δ (ppm) 8.95–7.97(m. 6H, NH$_2$, aromatic), 7.94–7.56(m,4H, aromatic), 6.21(s, 1H, CH), 3.97–3.90(m, 2H, CH$_2$), 0.99(t, 3H, J = 7.00Hz, Me).

Compound 5o: Yield: 84%, yellow powder; Mp. 256-258 °C (lit. 259-261 °C) [18]; FTIR (ν_{max}, cm^{-1}) 3436- 3326(NH$_2$ stretch), 1701(C=O stretch), 1617(C=O stretch), 1430–1617(arom. C=C stretch); ^{1}H NMR (400 MHz, DMSO-d_6) δ (ppm)
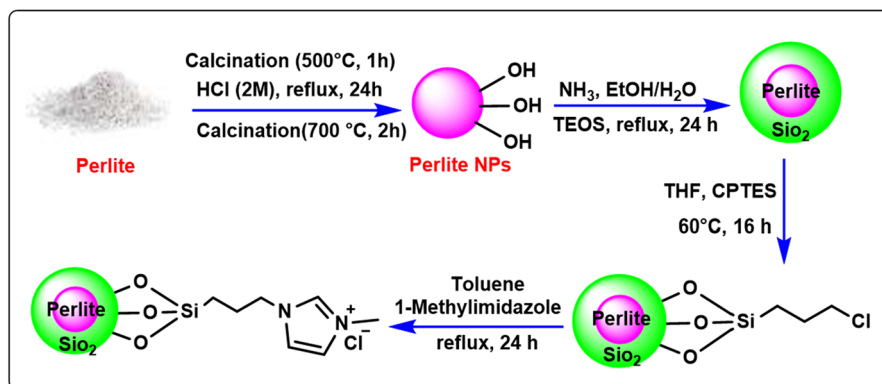
Scheme 1 The synthesis steps of the Perlite NPS/SiO$_2$/IL

8.29–7.28(m, 6H, NH$_2$, aromatic), 7.22–6.86(m, 4H, aromatic), 6.29(s, 1H, CH), 3.93(q, 2H, $J = 7.00$ Hz, CH$_2$), 3.63(s, 3H, OMe), 0.99(t, 3H, $J = 7.00$Hz, Me).

Compound 5p (Intermediate II): Yield: 91%, white powder; Mp. 230-232 °C (lit. 230-232 °C) [18]; FTIR (ν_{max}, cm^{-1}) 3321(N–H stretch), 1700(C=O stretch), 1646(arom. C=C stretch), 1486(N–H), 1346(C-H); ^{1}H NMR (400MHz, DMSO-*d6*) δ (ppm) 11.54 (2H, NH), 8.05 (d, $J = 6.0$ Hz, 2H, aromatic), 7.86 (t, $J = 6.0$ Hz, 2H, aromatic).

Results and discussion

The overall process of Perlite NPs/SiO$_2$/IL preparation is schematically represented in Scheme 1. After the successful preparation of Perlite NPs/SiO$_2$/IL through a three-step process, our initial effort was focused on accurate characterization using different analytical techniques.

Investigation of morphology

The FE-SEM images of the Perlite NPs, and Perlite NPS/SiO$_2$/IL are shown in Fig. 1. The image related to the prepared perlite nanoparticles (Fig. 1a, b) shows that the perlite particles are prepared in nano size. Comparing the image of primary nanoparticles and nanoparticles containing ionic liquid shows that there are no changes in the morphology and structure of primary nanoparticles (Fig. 1c, d). Moreover, the low and high-magnification TEM images of Perlite NPS/SiO$_2$/IL are shown in Fig. 2a, b. The TEM images of the catalyst show that the catalyst morphology is nearly lumpy and amorphous. Also, the elemental mapping from SEM measurements confirms that the Si, Al, K, Fe, Ca, Mg and atoms N are homogeneously dispersed (Fig. 3).
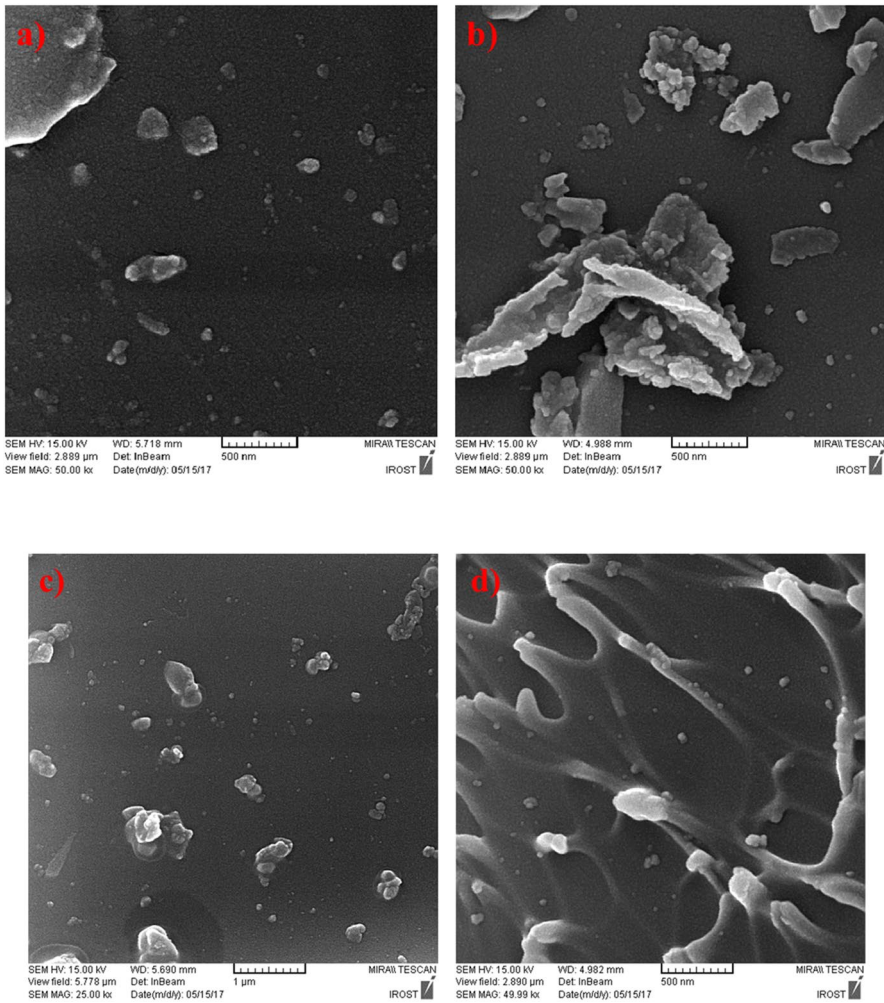
Fig. 1 FESEM illustrations of Perlite NPs (**a–b**), and Perlite NPs/SiO$_2$/IL (**c–d**)

The EDX analysis was performed for investigation of the successful immobilization of ionic liquid (IL) on the silica-coated nanosized perlite structure. Figure 4a shows the presence of Si, Al, K, Ca, Na, Mg, and O elements in the perlite nanoparticles structure. Moreover, the corresponding peak of N appeared in the EDX of Perlite NPs/SiO$_2$/ IL, indicating the presence of imidazolium ionic liquid on the silica-coated nanosized perlite structure (Fig. 4b).
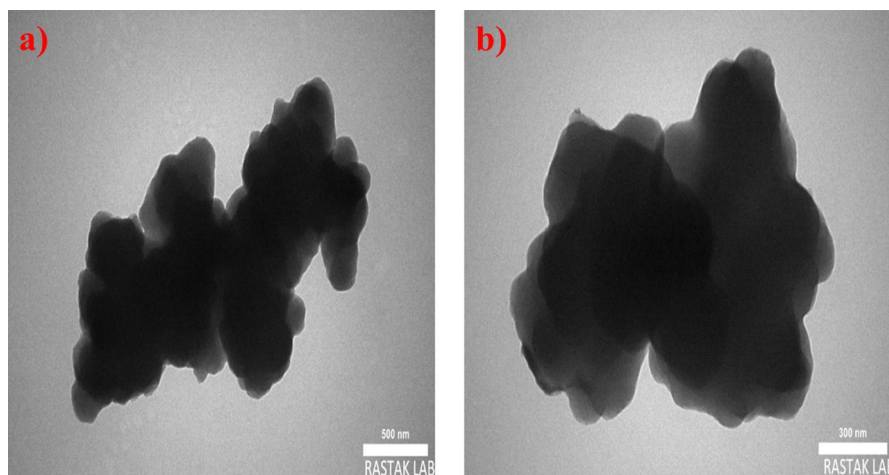
Fig. 2 TEM images of synthesized Perlite NPs/SiO$_2$/IL

XRD patterns

As seen in Fig. 5, the phase structures of the Perlite NPs and Perlite NPs/SiO$_2$/IL were confirmed by the XRD analysis. From the X-ray diffraction data obtained, it can be seen that perlite nanoparticles are amorphous. Also, no change in X-ray diffraction has been achieved after stabilizing the ionic liquid on the perlite nanoparticles.

TGA analysis

The thermal stability of synthesized Perlite NPs/SiO$_2$/IL was also investigated by TGA analysis The obtained results are displayed in Fig. 6. There are two major weight losses in the thermogram of NPs/SiO$_2$/IL at 88-164 °C and 211-439 °C that can be related to the removal of water molecules which have been adsorbed on the surface of the catalyst and the loss of the covalently attached organic groups on perlite surfaces respectively.

BET surface area

The N$_2$ adsorption–desorption isotherm of Perlite NPs/SiO$_2$/IL revealed a characteristic type IV curve with a typical H3 hysteresis loop (Fig. 7). The data obtained by BET measurements of the synthesized Perlite NPs/SiO$_2$/IL have been given in Table 1. The BET surface area of Perlite NPs/SiO$_2$/IL was found to be 9.1235 m^2/g, whereas the BJH adsorption surface area of pores was 2.3887 m^2/g. The single point
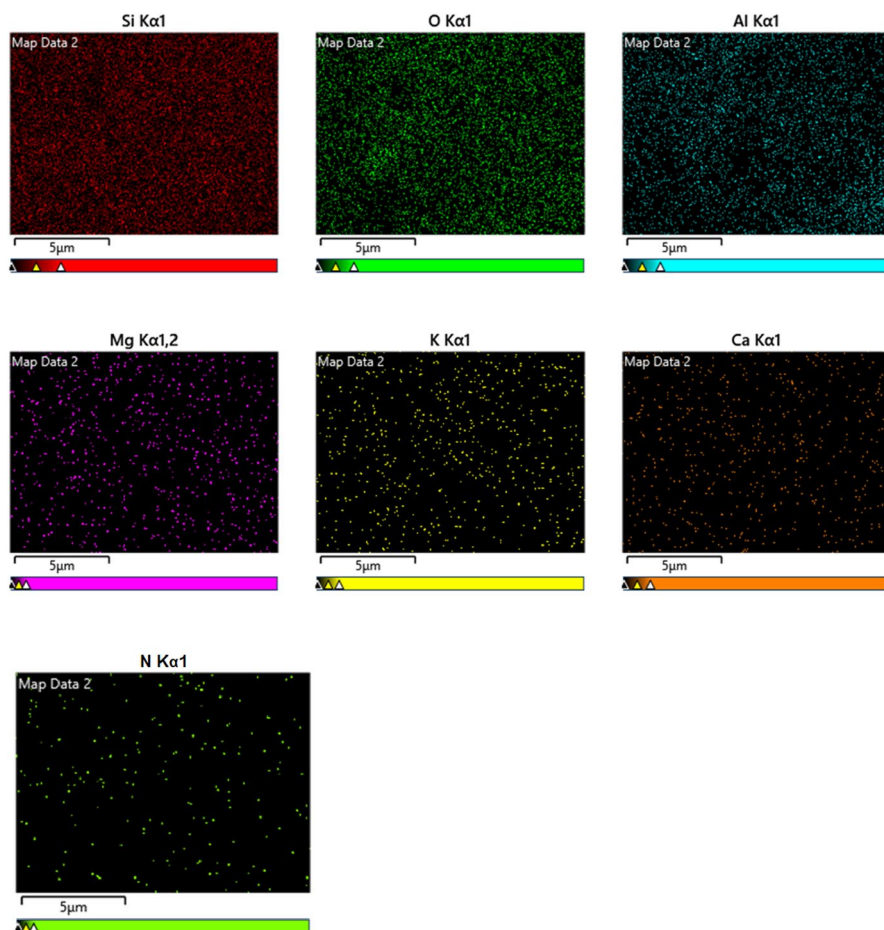
Fig. 3 The element mappings of Perlite NPs/SiO$_2$/IL

total pore volume was found to be 0.021094 cm^{3}g^{-1} and the pore diameter was 9.2483 nm.

The catalytic activity of Perlite NPs/SiO$_2$/IL in multicomponent reaction of the one-pot, four -component synthesis of 1H-pyrazolo [1,2-b] phthalazine-5,10-diones

After the successful preparation and characterization of Perlite NPs/SiO$_2$/IL as a new nanocatalyst, its catalytic activity was studied for the synthesis of 1H-pyrazolo [1,2-b] phthalazine-5,10-dione derivatives. To this regard, the reaction of phthalimide (**1a**, 1mmol), hydrazine hydrate (**2a**, 1 mmol), benzaldehyde (**3d**,
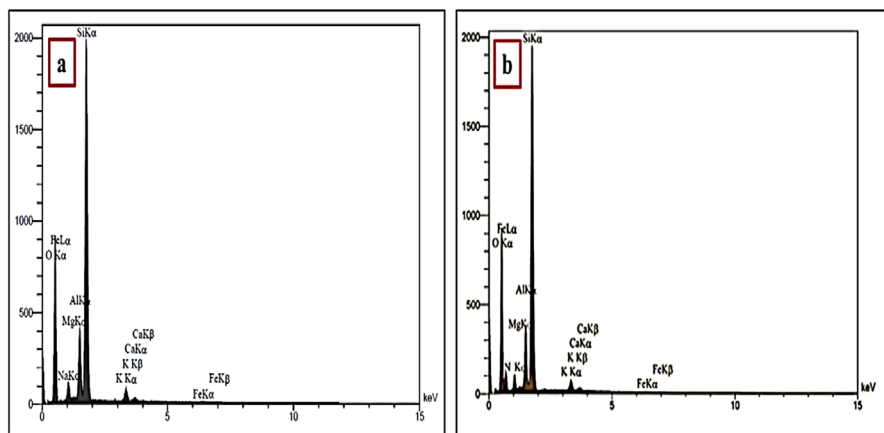
Fig. 4 EDX Spectra of Perlite NPs (**a**), and Perlite NPs/SiO₂/IL (**b**)
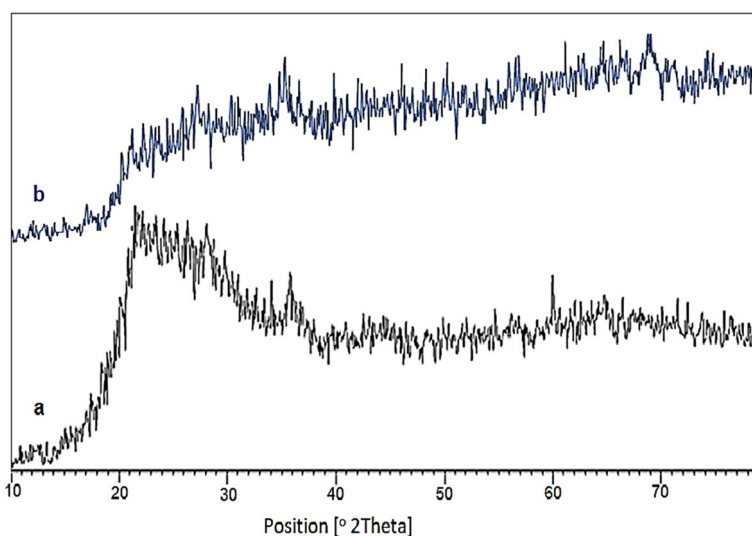

Fig. 5 XRD spectra of Perlite NPs (**a**), and Perlite NPs/SiO₂/IL (**b**)

1mmol) and malonitril (**4a**, 1mmol) was selected as a model reaction and the time and the yield of the reaction were monitored under different conditions such as solvent, temperature and the amount of catalyst and obtained results were summarized in Table 2. As it is clear from Table 2, moderate to good yields were obtained in H_2O: EtOH (1:1) and H_2O (entries 1 and 3), while the yield of the model reaction in CH_3CN and $CHCl_3$, was not effective and very low yields were obtained after a long time (8 h) (entries 4 and 5). The best results were
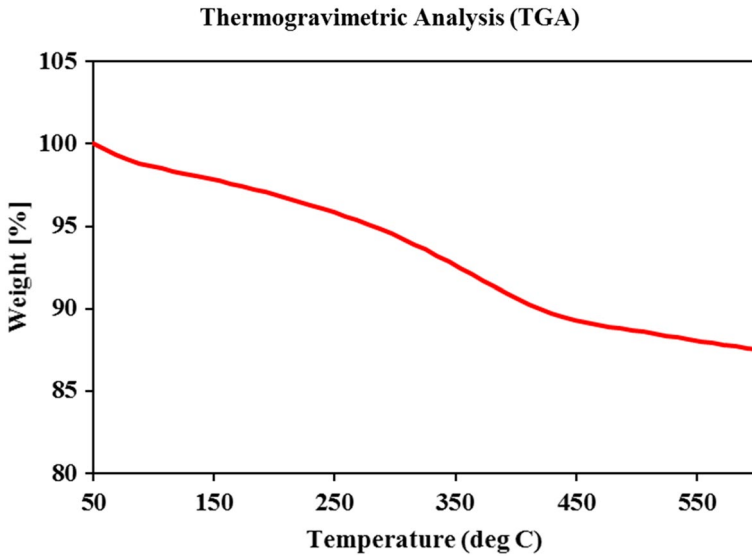
Thermogravimetric Analysis (TGA)

Fig. 6 Thermogravimetric analysis (TGA) diagrams of Perlite NPs/SiO$_2$/IL
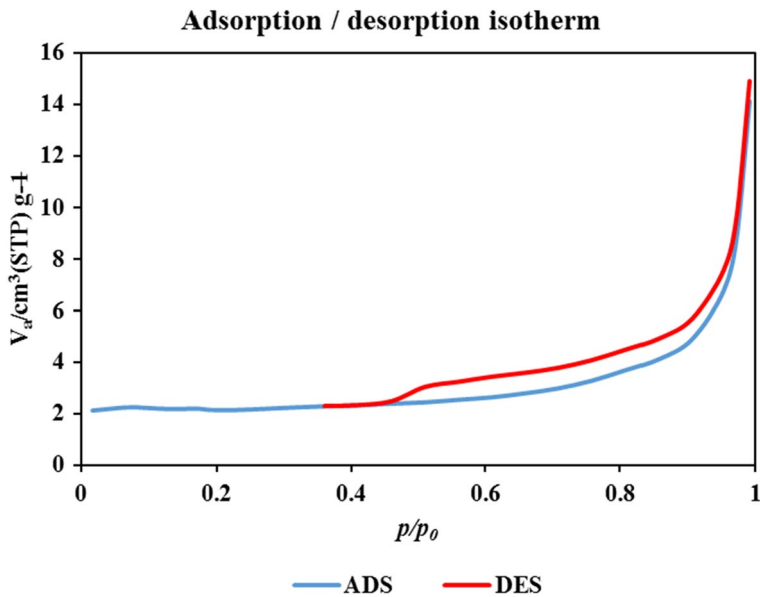
Adsorption / desorption isotherm

Fig. 7 Nitrogen adsorption – desorption isotherms of Perlite NPs/SiO$_2$/IL

Table 1 Results of BET surface area measurements for Perlite NPs/SiO$_2$/IL

BET	
V$_m$	2.0962 [cm^3(STP) g^{-1}]
a$_{s,BET}$	9.1235 [m^2 g^{-1}]
Total pore volume(p/p$_0$=0.990)	0.021094 [cm^3 g^{-1}]
Mean pore diameter	9.2483 [nm]
BJH	
Plot data	Adsorptionbranch
V$_p$	0.018811 [cm^3 g^{-1}]
r$_{p,peak}$(*Area*)	4.65 [nm]
a$_p$	2.3887 [m^2 g^{-1}]

obtained using 0.02 g of the catalyst in ethanol (entry 8), and the increasing the catalyst quantity did not exhibit a significant effect on the reaction time and yield (entries 9 and 10), whereas the decrease in the quantity of catalyst was lead to a significant increase of reaction times and decrease of the yields (entry 7). As the results indicate, the reaction is highly sensitive to the presence of the catalyst and did not proceed without the catalyst even after a long time (24 h) (entry 11). Furthermore, the reaction temperature directly affects the yield and time of the reaction. The shortest reaction time (4.0 h) and the best reaction yield (88%) were obtained at 78 °C (entry 8). Increasing the temperature up to 90 °C had no significant effect on the time and yield of the reaction (entry 13). However, lowering the temperature significantly increased reaction time and decreased the yield (entry 12). Therefore, considering all of these results, the best reaction conditions for the reaction of phthalimide (**1a**), hydrazine hydrate (**2a**), benzaldehyde (**3d**) and malononitrile (**4a**) in the presence of PerliteNPs/SiO$_2$/IL is the use of EtOH (2.0 mL) as a solvent, 0.02 g of the catalyst and conduction of the reaction at 78 °C.
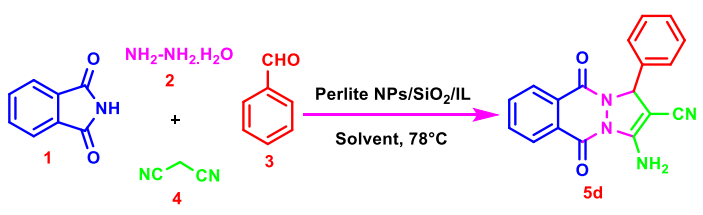
Encouraged by the remarkable optimization results, we decided to use phthalimide (**1a**), hydrazine hydrate (**2a**), various aryl aldehydes (**3a-o**) and malononitrile (**4a**), to test the scope, efficiency and generality of the synthesis of 1H-pyrazolo [1,2-b] phthalazine-5,10-dione derivatives (**5a-o**) in the presence of PerliteNPs/SiO$_2$/IL as a new and reusable catalyst under optimized conditions. The obtained results are exhibited in Table 3. As can be seen, aromatic aldehydes with electron-withdrawing groups reacted faster than those with electron-releasing groups.

Reusability, kinetic studies, hot filtration test

Having established the efficacy of Perlite NPs/SiO$_2$/IL in the synthesis of compound **5d**, we then investigated the catalyst recyclability in the reaction (Fig. 8a). Upon completion of the reaction, the Perlite NPs/SiO$_2$/IL catalyst was separated

from the reaction mixture using filtration, washed with ethanol, and reused in the next run after drying at 80 °C for 6 h. The model reaction was run six times with the use of recovered Perlite NPs/SiO$_2$/IL in each run without considerable loss of the catalytic activity (Fig. 8a). Besides, the chemical and physical stabilities of the nanocatalyst were investigated after the 6th reuse with XRD and FESEM analyses (Fig. 8b, c). The XRD pattern of the recovered catalyst after the 6th reuse (Fig. 8b) is completely similar to the freshly synthesized catalyst (Fig. 5b) and indicates the stability of the chemical structure of the catalyst. Moreover, there is no difference between the FESEM image of freshly synthesized (Fig. 1c, d) and the recovered catalyst after the 6th reuse (Fig. 8c) and based on the FESEM image of the recovered catalyst (Fig. 8c) significant changes were not observed in the morphology of the surface of the nanocatalyst. We found that no impurities entered in our catalytic system and the products and starting materials were completely separated from the catalyst.

Table 2 Optimization of the reaction conditions for the synthesis of model reaction

Entry	Solvent	Catalyst amount (g)	Temperature (°C)	Time (h)	Yield (%)[a]
1	H$_2$O	0.01	78	5:00	65
2	EtOH	0.01	78	5:00	88
3	H$_2$O/EtOH (1:1)	0.01	78	5:00	75
4	CH$_3$CN	0.01	78	8:00	55
5	CHCl$_3$	0.01	78	8:00	52
6	–	0.01	78	12:00	–
7	EtOH	0.009	78	7:00	60
8	**EtOH**	**0.02**	**78**	**4:00**	**88**
9	EtOH	0.03	78	4:00	75
10	EtOH	0.05	78	4:00	75
11	EtOH	-	78	24.00	-
12	EtOH	0.02	70	6:00	65
13	EtOH	0.02	90	4:00	60

[a]*Reaction conditions:* phthalimide (**1a**), hydrazine hydrate (**2a**), benzaldehyde (**3d**), and malononitrile (**4a**), PerliteNPs/SiO$_2$/IL catalyst (g) and solvent (2.0 mL)

[b]Isolated yields

The kinetic study of perlite NPs/SiO$_2$/IL as a heterogeneous catalyst in the formation of compound **5d** implies that the catalyst is active and catalyzes the reaction similarly from the beginning to the end for all six runs, as it can be found in Fig. 9.

We have carried out the hot filtration test to investigate the heterogeneous nature of Perlite NPs/SiO$_2$/IL (Fig. 10). Initially, a mixture of phthalimide (**1a**), hydrazine hydrate (**2a**), benzaldehyde (**3d**) and malononitrile (**4a**) 0.02 g of Perlite NPs/SiO$_2$/IL, Ethanol (2 mL) at 78 °C, were put it on the steerer for 2 h. The model reaction was quenched after 2 h (with 41% formation of 5d) and the catalyst was removed. The reaction mixture was then centrifuged for 10 min and the catalyst was separated from the solution. The solution was put on the steerer for another 2 h under the same conditions as before. Again after 2 h, the reaction efficiency was checked which was 47% of the reaction efficiency, and no improvement was shown in the reaction which indicated that the catalyst has heterogeneous behavior and the progress of the reaction depended on the use of the catalyst.

Mechanism study

A plausible mechanistic pathway was proposed for the four-component reaction of phthalimide (**1**), hydrazine hydrate (**2**), benzaldehyde (**3a**) and malononitrile (**4**), in the presence of Perlite NPs/SiO$_2$/IL as an efficient separable catalyst (Scheme 2) [18, 86]. As shown in Scheme 2, Perlite NPs/SiO$_2$/IL, increases the electrophilicity of the carbonyl group of aldehyde. Then, intermediate **I** is formed by the condensation of malononitrile anion with activated benzaldehyde. On the other hand, intermediate **II** is created by the reaction of phthalimide with hydrazine in the presence of the catalyst and removing NH$_3$. After that, Intermediate **III** is formed by Michael addition between intermediate **I** and **II**. Next, the final product is produced by cyclization and tautomerization of intermediate **III**.

Finally, to evaluate the efficiency of the perlite NPs/SiO$_2$/IL as a new highly efficient and reusable catalyst, its activity in the multicomponent reaction of phthalimide (**1**), hydrazine hydrate (**2**), benzaldehyde (**3d**) and malononitrile (**4a**) was compared with some other catalysts, which have been reported previously. The gathered data in Table 4 showed that the reaction was performed in a shorter reaction time using perlite NPs/SiO$_2$/IL and produced the desired product (**5d**) in excellent yield. Another important advantage of the introduced nanocatalyst is the facile separation from the reaction medium and reusability.
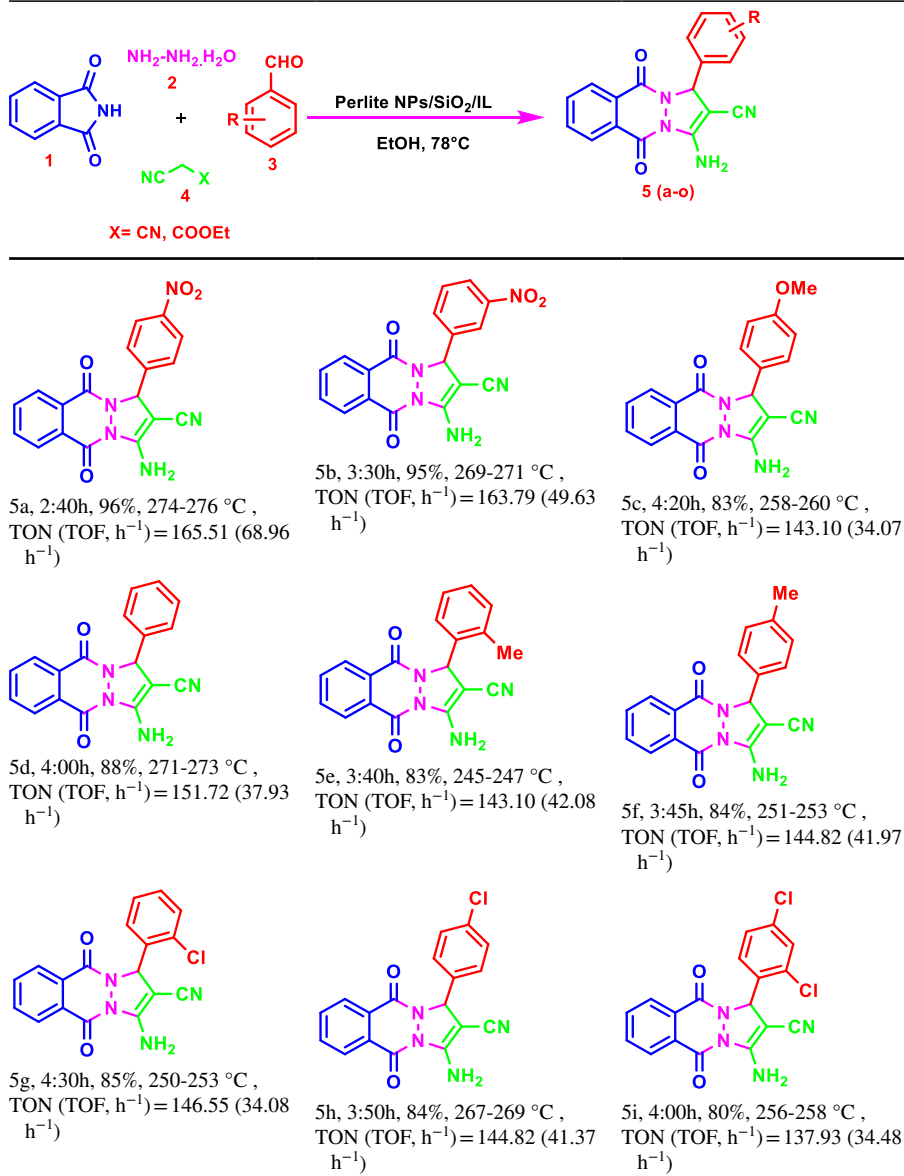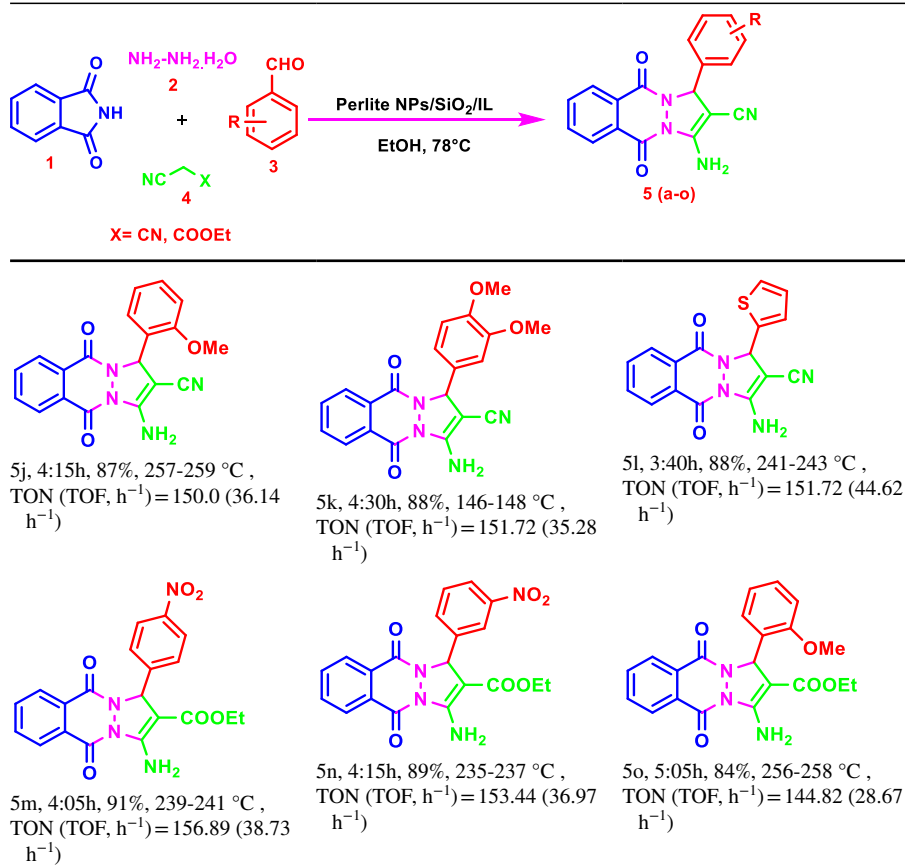
Table 3 Catalyzed synthesis of 1H-pyrazolo [1,2-b] phthalazine-5,10-dione derivatives in the presence of Perlite NPs/SiO₂/IL

5a, 2:40h, 96%, 274-276 °C , TON (TOF, h⁻¹) = 165.51 (68.96 h⁻¹)

5b, 3:30h, 95%, 269-271 °C , TON (TOF, h⁻¹) = 163.79 (49.63 h⁻¹)

5c, 4:20h, 83%, 258-260 °C , TON (TOF, h⁻¹) = 143.10 (34.07 h⁻¹)

5d, 4:00h, 88%, 271-273 °C , TON (TOF, h⁻¹) = 151.72 (37.93 h⁻¹)

5e, 3:40h, 83%, 245-247 °C , TON (TOF, h⁻¹) = 143.10 (42.08 h⁻¹)

5f, 3:45h, 84%, 251-253 °C , TON (TOF, h⁻¹) = 144.82 (41.97 h⁻¹)

5g, 4:30h, 85%, 250-253 °C , TON (TOF, h⁻¹) = 146.55 (34.08 h⁻¹)

5h, 3:50h, 84%, 267-269 °C , TON (TOF, h⁻¹) = 144.82 (41.37 h⁻¹)

5i, 4:00h, 80%, 256-258 °C , TON (TOF, h⁻¹) = 137.93 (34.48 h⁻¹)

Table 3 (continued)

5j, 4:15h, 87%, 257-259 °C , TON (TOF, h^{-1}) = 150.0 (36.14 h^{-1})

5k, 4:30h, 88%, 146-148 °C , TON (TOF, h^{-1}) = 151.72 (35.28 h^{-1})

5l, 3:40h, 88%, 241-243 °C , TON (TOF, h^{-1}) = 151.72 (44.62 h^{-1})

5m, 4:05h, 91%, 239-241 °C , TON (TOF, h^{-1}) = 156.89 (38.73 h^{-1})

5n, 4:15h, 89%, 235-237 °C , TON (TOF, h^{-1}) = 153.44 (36.97 h^{-1})

5o, 5:05h, 84%, 256-258 °C , TON (TOF, h^{-1}) = 144.82 (28.67 h^{-1})

Reaction conditions phthalimide (**1a**), hydrazine hydrate (**2a**), various aryl aldehydes (**3d**) and malononitrile (**4a**) in the presence of 0.02 g of perlite NPs/SiO$_2$/IL in EtOH (2.0 mL) at 78 °C

Isolated yields

Conclusions

In summary, the imidazole based ionic liquid (IL) immobilized on the silica-coated nanosized perlite as a new separable and reusable catalyst was designed, successfully synthesized, and fully characterized with various techniques. After-wards, the prepared catalyst was applied for the synthesis of 1H-pyrazolo [1,2-b] phthalazine-5,10-diones in ethanol at 78 °C. The target products were obtained in high to excellent yields (80–96%) in this protocol. Moreover, the results of hot filtration studies show the lack of IL leaching from the catalyst surfaces and prove
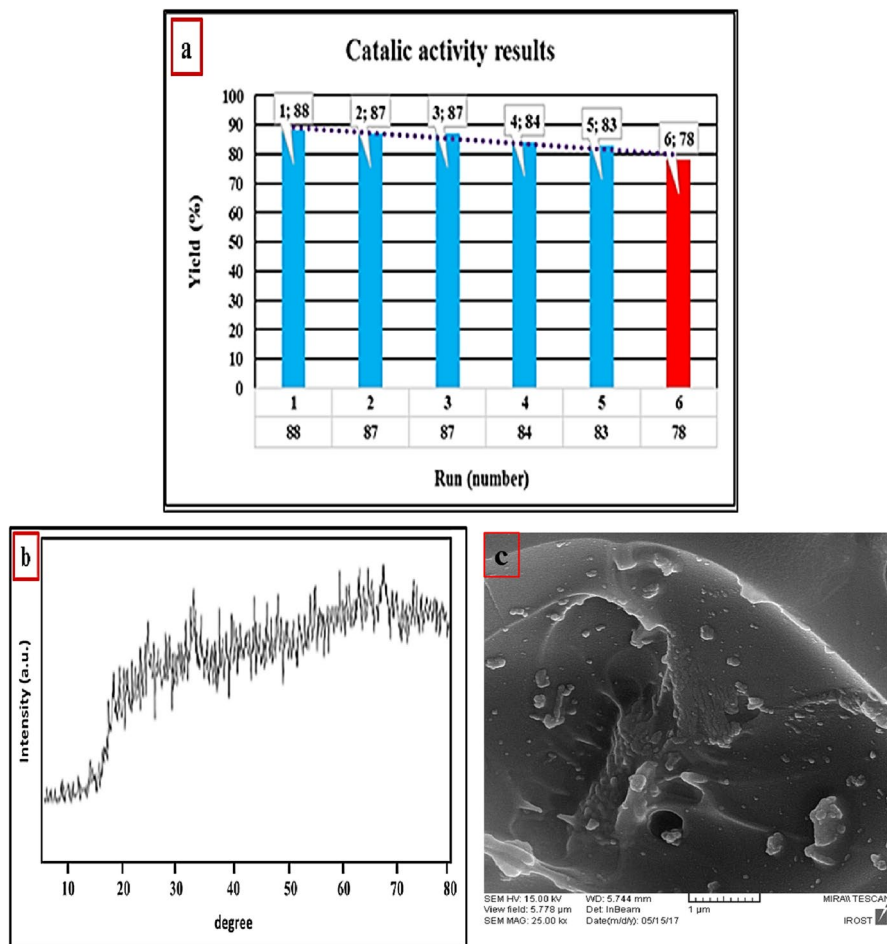
Fig. 8 a The recycling of catalyst for the direct synthesis of compound **5d**; **b** XRD pattern; **c** FESEM image of recovered perlite NPs/SiO$_2$/IL after the 6th run

the complete heterogeneous property of perlite NPs/SiO$_2$/IL, for catalyzing the reaction under optimized conditions. The most promising points for the presented methodology are operational simplicity, mild reaction conditions, no formation of by-products, chemical stability of the catalyst, easy workup, clean reaction profile, environmentally benign solvent, enhanced rates and agreement with some of the green chemistry aspects.
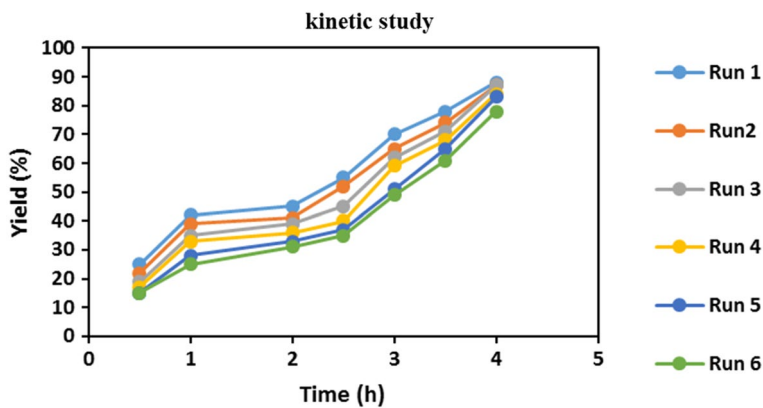
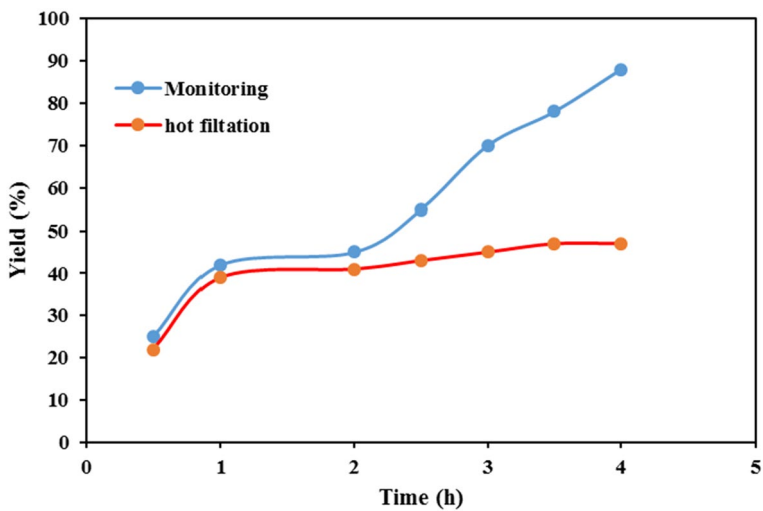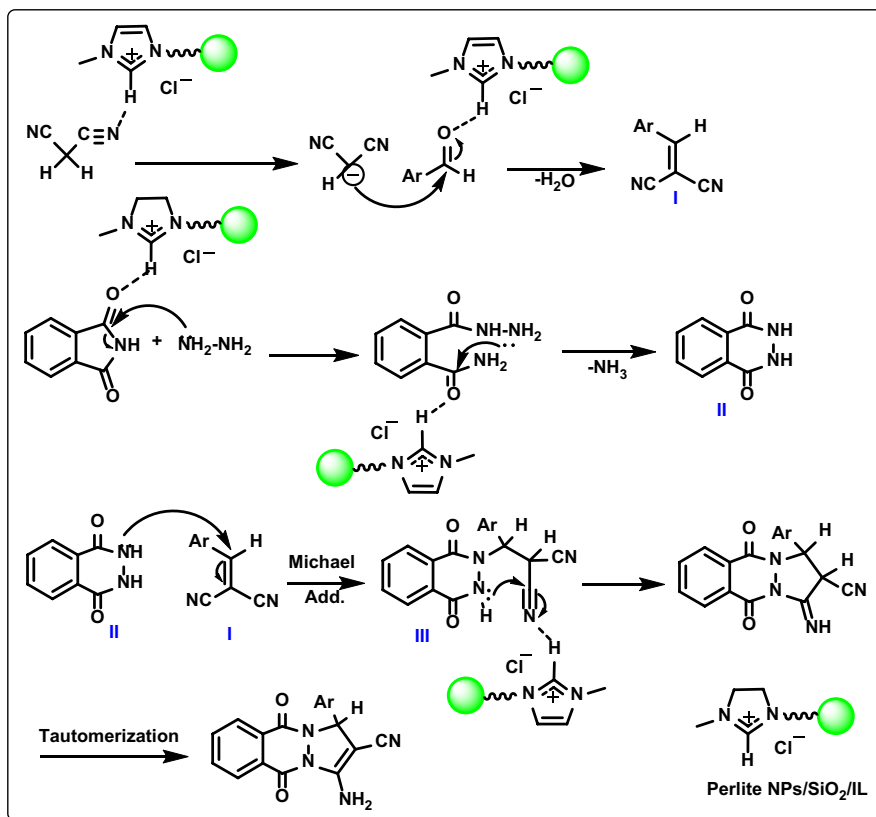**Fig. 9** kinetic study of formation of compound **5d**

Fig. 10 Monitoring and hot filtration test in the catalyzed multicomponent synthesis of **5d**

Scheme 2 The plausible mechanistic pathway for the synthesis of compound **5d** in the presence of in the presence of perlite NPs/SiO$_2$/IL

Table 4 The comparison of perlite NPs/SiO$_2$/IL catalytic activity with some reported catalysts for the preparation of compound **5d**[a]

Entry	Catalyst	Conditions	Time (h)	Yield (%)
1	ZrO$_2$ nanoparticles	Solvent-free, 100 °C	0.66	91 [35]
2	NiCl$_2$ 6H$_2$O	Ethanol, reflux	3	87[28]
3	TBBD [b]	Ethanol, 100 °C	0.25	89[83]
4	Triethylamine	Ethanol, 50 °C , U.S	1	90[84]
5	p-Toluenesulfonic acid	[BMIM] Br, 100 °C	3	94[17]
6	APTES-MNPs	Solvent-free, r.t	0.31	92[34]
7	NiFe$_2$O$_4$-TiO$_2$/ piperazine	PEG 400, 80 °C	1	94[32]
8	[Bn-DBU][TFA]	Solvent-free, 100 °C	0.133	92[28]
9	Fe$_3$O$_4$@Cu(II) Schiff base	Solvent-free, 80 °C	0.16	96[85]
10	NiFe$_2$O$_4$-TiO$_2$/piperidin-4-NH$_4$I	Solvent-free, 80 °C	0.75	95[32]
11	AL-KIT-6	Ethanol, 60 °C	4	93[24]
12	CuI nanoparticles	Solvent-free, 70 °C	0.45	91[30]
13	Theophylline	Solvent-free, 70 °C	2	85[26]
14	[bmim]OH	Ethanol, 60 °C	0.8	98[74]
15	Cu-Doped ZnO	Solvent-free, 100 °C	0.13	93[75]
16	K$_2$CO$_3$	Ethanol, reflux	1.16	86[76]
17	DBU	Solvent-free, 78 °C	3	87[77]
18	STA-Amine-Si-MNPs	Methanol, reflux	0.33	90[78]
19	Saccharin	Solvent-free, 90 °C	3	89[80]
20	Perlite/SiO$_2$/guanidine	Ethanol, 78 °C	2.66	97[18]
21	Perlite NP@IL/ZrCl$_4$	Ethanol, 78 °C	6	89
22	Perlite/SiO$_2$/IL[c]	Ethanol, 78 °C	4	96

[a]*Reaction conditions*: phthalimide (**1**, 1 mmol), hydrazine hydrate (**2**, 1 mmol), Benzaldehyde (**3d**, 1 mmol). malononitrile (**4a**, 1 mmol)

[b]Tetrabromobenzene-1,3-disulfonamide/Polybrominated biphenyl

[c]Current work

Author contributions Leila Moradi:Supervision, Original idea, Conceptualization, Validation, Review & editing. Hamideh Rouhi Sasi: Investigation, Methodology,Performing of experimental tests, Abdulhamid Dehghani: Investigation,Validation, Writing.

Declarations

Competing interests The authors declare no competing interests.

References

1. M. Hossain, A.K, Nanda, Science. **6:**83–94 (2018)
2. A.M. Bistgani, A. Dehghani, L. Moradi, RSC Adv. **13**, 35781–35790 (2023)
3. M. Dehnavian, A. Dehghani, L. Moradi, RSC Adv. **12**, 25194–25203 (2022)
4. W. Guo, M. Zhao, W. Tan, L. Zheng, K. Tao, X. Fan, Org. Chem. Front. **6**, 2120–2141 (2019)
5. H. Li, H. Guo, Z. Fang, T.M. Aida, R.L. Smith, Green Chem. **22**, 582–611 (2020)
6. Y. Delshad, A. Dehghani, M. Ghezelsofloo, S. Ghasemi, Chem. Res. Nanomater. **4**, 25 (2022)
7. A. Moazeni Bistgani, A. Dehghani, L. Moradi, Chem. Res. Nanomater. **2**, 20 (2022)
8. V.V. Chernyshov, I.I. Popadyuk, O.I. Yarovaya, N.F. Salakhutdinov, Top. Curr. Chem. **380**, 42 (2022)
9. J. Qiao, X. Jia, P. Li, X. Liu, J. Zhao, Y. Zhou, F. Zhao, Adv. Synth. Catal. **361**, 1419–1440 (2019)
10. F. Ghobakhloo, D. Azarifar, M. Mohammadi, H. Keypour, H. Zeynali, Inorg. Chem. **61**, 4825–4841 (2022)
11. M. Kazemi, M. Mohammadi, M. Appl, Organomet. Chem. **34**, 5400 (2020)
12. J. Sangshetti, S.K. Pathan, R. Patil, S.A. Ansari, S. Chhajed, R. Arote, D.B. Shinde, Bioorg. Med. Chem. **27**, 3979–3997 (2019)
13. M. Asif, Curr. Med. Chem. **19**, 2984–2991 (2012)
14. A.M. Khalil, M.A. Berghot, M.A. Gouda, Eur. J. Med. Chem. **44**, 4448–4454 (2009)
15. F. Mohamadpour, M.T. Maghsoodlou, R. Heydari, M. Lashkari, Res. Chem. Intermed. **42**, 7841–7853 (2016)
16. Y. Su, W. Xu, F. Qiu, D. Wu, P., Liu, M., Xue, F. Zhang, Chin. J. Chem. **31**, 1397–1403 (2013)
17. R. Ghahremanzadeh, G.I. Shakibaei, A. Bazgir, Synlett **2008**, 1129–1132 (2008)
18. L. Moradi, M. Mirzaei, H.R. Sasi, J. Mol. Struct. **1263**, 133124 (2022)
19. S. Grasso, G. De Sarro, A. De Sarro, N. Micale, M. Zappalà, G. Puja, C. De Micheli, J. Med. Chem. **43**, 2851–2859 (2000)
20. N. Watanabe, Y. Kabasawa, Y. Takase, M. Matsukura, K. Miyazaki, H. Ishihara, H. Adachi, J. Med. Chem. **41**, 3367–3372 (1998)
21. R.E. Khidre, M.S. Mostafa, Y.E. Mukhrish, M.A. Salem, M.S. Behalo, Curr. Org. Chem. **26**, 2055–2069 (2022)
22. A.A. Bekhit, H.T. Rostom, S.A. Fahmy, A.M. Baraka, Eur. J. Med. Chem. **38**, 27–36 (2003)
23. W.M. Eldehna, H. Almahli, G.H. Al-Ansary, H.A. Ghabbour, M.H. Aly, O.E. Ismael, H.A. Abdel-Aziz, J. Enzyme Inhib. Med. Chem. **32**, 600–613 (2017)
24. G. Karthikeyan, A. Pandurangan, J Mol Catal A Chem. **361**, 58–67 (2012)
25. M.V. Reddy, Y.T. Jeong, Tetrahedron Lett. **54**, 3546–3549 (2013)
26. F. Mohamadpour, Org. Prep. Proced. Int. **52**, 64–68 (2020)
27. A. Ghorbani-Choghamarani, M. Mohammadi, T. Tamoradi, M. Ghadermazi, Polyhedron **158**, 25–35 (2019)
28. A.M. Bistgani, L. Moradi, A. Dehghani, Catal. Commun. **182**, 106755 (2023)
29. S.H. Song, J. Zhong, Y.H. He, Z. Guan, Tetrahedron Lett. **53**, 7075–7077 (2012)
30. J. Safaei-Ghomi, H. Shahbazi-Alavi, A. Ziarati, R. Teymuri, M.R. Saberi, Chin. Chem. Lett. **25**, 401–405 (2014)
31. R. Ghorbani-Vaghei, J. Mahmoodi, Y. Maghbooli, Appl. Organomet. Chem. **31**, 3717 (2017)
32. M. Hamidinasab, M.A. Bodaghifard, A. Mobinikhaledi, Appl. Organomet. Chem. **34**, 5386 (2020)
33. M. Hamidinasab, A. Ameri, A. Hekmat, H. Forootanfar, T. Mortezazadeh, M.A. Bodaghifard, M. Khoobi, Bioorg. Med. Chem. **30**, 115944 (2021)
34. H.R. Shaterian, M. Mohammadnia, Res. Chem. Intermed. **40**, 371–383 (2014)
35. M. Piltan, Heterocycl. Commun. **23**, 401–403 (2017)
36. M. Kour, M. Bhardwaj, H. Sharma, S. Paul, J.H. Clark, New J. Chem. **2017**(41), 5521–5532 (2017)
37. M. Hosseini-Sarvari, F. Jafari, A. Dehghani, Appl. Nanosci. **12**, 2195–2205 (2022)
38. M. Toorbaf, L. Moradi, A. Dehghani, J. Mol. Struct. **1294**, 136335 (2023)
39. M. Hosseini-Sarvari, A. Dehghani, Monatsh. Chem. **154**, 397–405 (2023)
40. A. Ghorbani-Choghamarani, M. Mohammadi, L. Shiri, Z. Taherinia, Res. Chem. Intermed. **45**, 5705–5723 (2019)
41. M. Mohammadi, A. Ghorbani-Choghamarani, S.M. Ramish, J. Mol. Struct. **1292**, 136115 (2023)

42. M. Norouzi, N. Noormoradi, M. Mohammadi, Nanoscale Adv **5**, 6594–6605 (2023)
43. L.D. Maxim, R. Niebo, E.E. McConnell, Inhal. Toxicol. **26**, 259–270 (2014)
44. M. Arifuzzaman, H.S. Kim, Constr Build Mate. **141**, 201–215 (2017)
45. D. Shastri, H.S. Kim, Constr. Build. Mater. **60**, 1–7 (2014)
46. S.F. Torabi, K. Khajeh, S. Ghasempur, N. Ghaemi, S.O.R. Siadat, J. Biotechno. **131**, 111–120 (2007)
47. A. Rostami-Vartooni, M. Nasrollahzadeh, M. Alizadeh, J. Alloys Compd. **680**, 309–314 (2016)
48. M. Esmaielpour, B. Akhlaghinia, R. Jahanshahi, J. Chem. Sci. **129**, 313–328 (2017)
49. B.A. Babazadeh, J. Razeghi, S. Jafarirad, R. Motafakkerazad, Ecotoxicology **30**, 899–913 (2021)
50. L. Moradi, M. Mirzaei, RSC Adv. **9**, 19940–19948 (2019)
51. T. Welton, Green Chem. **13**, 225–225 (2011)
52. S.V. Dzyuba, K.D. Kollar, S.S. Sabnis, J. Chem. Educ. **86**, 856 (2009)
53. S. Sadjadi, J. Mol. Liq. **323**, 114994 (2021)
54. A. Stark, D. Ott, D. Kralisch, G. Kreisel, B. Ondruschka, J. Chem. Educ. **87**, 196–201 (2010)
55. I. Newington, J.M. Perez-Arlandis, T. Welton, Org. Lett. **9**, 5247–5250 (2007)
56. J.L. Anderson, D.W. Armstrong, G.T. Wei, Anal. Chem. **78**, 2892–2902 (2006)
57. E.E. Tanner, A.M. Curreri, J.P. Balkaran, N.C. Selig-Wober, A.B. Yang, C. Kendig, S. Mitragotri, Adv. Mater. **31**, 1901103 (2019)
58. B. Rotenberg, O. Bernard, J.P. Hansen, J. Condens, Matter Phys. **30**, 054005 (2018)
59. C.P. Fredlake, J.M. Crosthwaite, D.G. Hert, S.N. Aki, J.F. Brennecke, J. Chem. Eng. Data **49**, 954–964 (2004)
60. B. Nuthakki, T.L. Greaves, I. Krodkiewska, A. Weerawardena, M.I. Burgar, R.J, Mulder, C.J. Drummond, Aust. J. Chem. **60**, 21–28 (2007)
61. T. Welton, Coord. Chem. Rev. **248**, 2459–2477 (2004)
62. H.P. Steinrueck, P. Wasserscheid, CATAL LETT. **145**, 380–397 (2015)
63. H. Olivier-Bourbigou, L. Magna, D. Morvan, Appl. Catal. A: Gen. **373**, 1–56 (2010)
64. K. Ghandi, Green Sustain. Chem. **2014** (2014)
65. K. Ueno, H. Tokuda, M. Watanabe, Phys. Chem. Chem. Phys. **12**, 1649–1658 (2010)
66. A.R. Hajipour, F. Rafiee, J. Iran. Chem. Soc. **6**, 647–678 (2009)
67. Y. Deng, F. Shi, J. Beng, K. Qiao, J Mol Catal A Chem. **165**, 33–36 (2001)
68. C.M. Gordon, Appl. Catal. A: Gen. **222**, 101–117 (2001)
69. B.C. Ranu, S. Banerjee, R. Jana, Tetrahedron **63**, 776–782 (2007)
70. I.A. Andreev, N.K. Ratmanova, A.U. Augustin, O.A. Ivanova, I.I., Levina, V.N. Khrustalev I.V. Trushkov, Angew. Chem., Int. Ed. **60**, 7927–7934 (2021)
71. H. Wender, L.F. de Oliveira, P. Migowski, A.F. Feil, E. Lissner, M.H. Prechtl, J. Dupont, J. Phys. Chem. C **114**, 11764–11768 (2010)
72. R. Tatumi, H. Fujihara, Chem comm **1**, 83–85 (2005)
73. F. Jia, C. Shan, F. Li, L. Niu, Biosens. Bioelectron. **24**, 945–950 (2008)
74. W. Wang, L. Cong-Hao, Y. Yi, L. Xiao-Jun, G. Hong-Yun, J. Chem. Res. **40**, 354–357 (2016)
75. B. Maleki, R. Nejat, H. Alinezhad, S.M. Mousavi, B. Mahdavi, M. Delavari, Org. Prep. Proced. Int. **52**, 328–339 (2020)
76. M. Abdesheikhi, Z. Karimi-Jaberi, J. Chem. Res. **39**, 482–483 (2015)
77. F. Mohamadpour, Indian J. Chem. Sect. B **59**, 1234–1242 (2020)
78. P. Arora, J.K. Rajput, Appl. Organomet. Chem. **32**, 4001 (2018)
79. H. Kefayati, S.H. Amlashi, R. Kazemi-Rad, A. Delafrooz, C. R. Chim. **17**, 894–898 (2014)
80. F. Mohamadpour, M.T. Maghsoodlou, R. Heydari, M. Lashkari, J. Iran. Chem. Soc. **13**, 1549–1560 (2016)
81. G.M. Ziarani, N.H. Mohtasham, A. Badiei, N. Lashgari, J. Chin. Chem. Soc. **61**, 990–994 (2014)
82. H.N. Roy, M. Rana, A.Z.A. Munsur, K.I. Lee, A.K. Sarker, Synth. Commun. **46**, 1370–1376 (2016)
83. R. Ghorbani-Vaghei, S. Noori, Z. Toghraei-Semiromi, Z. Salimi, RSC Adv. **4**, 47925–47928 (2014)
84. M.R. Nabid, S.J.T. Rezaei, R. Ghahremanzadeh, A. Bazgir, Ultrason. Sonochem. **17**, 159–161 (2010)
85. H. Ebrahimiasl, D. Azarifar, M. Mohammadi, H. Keypour, M. Mahmood abadi, Res. Chem. Intermed. **47**, 683–707 (2021)
86. Y. Tao, R. Dong, I.V. Pavlidis, B. Chen, T. Tan, Green Chem. **18**, 1240–1249 (2016)